The urogynecological side of pelvic floor MRI: the clinician's needs and the radiologist's role

Rania Farouk El Sayed

Abdominal Imaging

ISSN 0942-8925
Volume 38
Number 5

Abdom Imaging (2013) 38:912-929
DOI 10.1007/s00261-012-9905-3

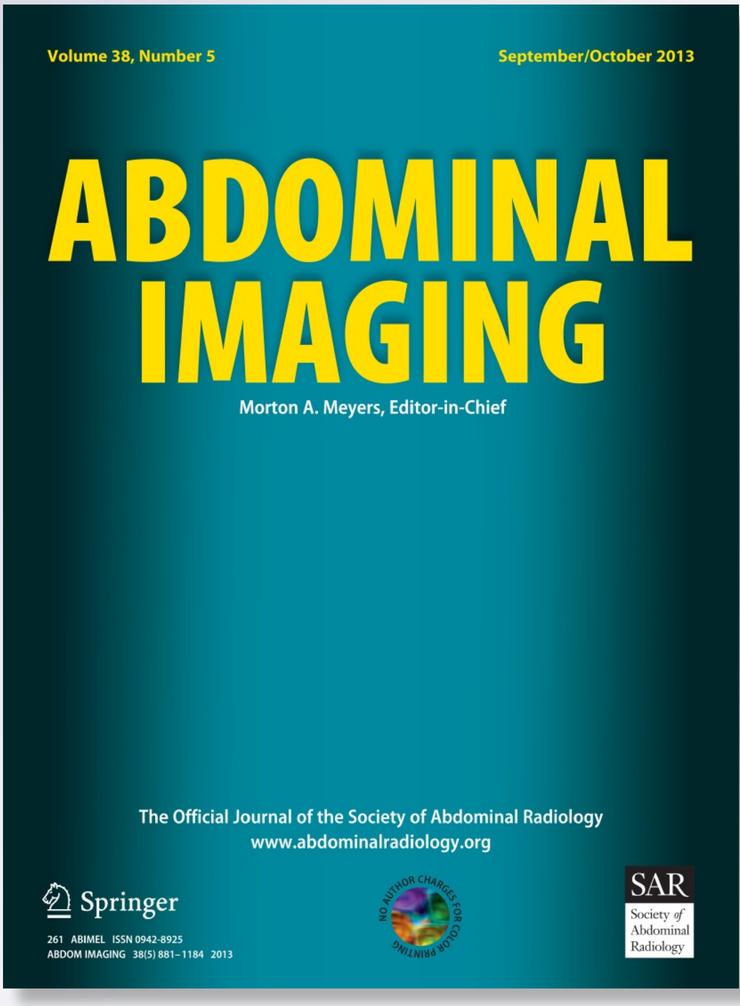

Springer

Abdominal Imaging

Published online: 1 June 2012

Abdom Imaging (2013) 38:912–929
DOI: 10.1007/s00261-012-9905-3

The urogynecological side of pelvic floor MRI: the clinician's needs and the radiologist's role

Rania Farouk El Sayed

Department of Radiology, Faculty of Medicine, Cairo University, Kaser El Aini, Naser City, Cairo 11511, Egypt

Abstract

In pelvic floor dysfunction (PFD), magnetic resonance imaging of the pelvic floor supporting system from a functional point of view allows radiologists to recognize and classify the types of defects in each supporting structure (namely, the urethral supporting system, the vaginal supporting system, and the anal sphincter complex). Combined analysis of both the static and dynamic images of patients reporting stress urinary incontinence and pelvic organ prolapse has revealed a close relationship between certain anatomical defects in the pelvic organ support system and specific PFD. Because of the consistency and reproducibility of this relationship, radiologists can accurately identify and report the underlying structural defects, allowing clinicians to individually tailor surgical techniques for each patient. This is important because even those patients presenting with the same clinical symptoms may have different underlying structural derangement or abnormalities that may warrant a different treatment plan or approach. In view of the reported high rate of dysfunction recurrence after surgical treatment and clinicians' desire for a test that can pinpoint each patient's structural and anatomical defects, this approach provides the necessary scientific evidence on which best clinical practice can be based, and the data-reporting system used for analysis provides a tool for accurately planning reconstructive surgery, reducing the risk of surgical failure, dysfunction recurrence, and reoperation. With the improved radiological evidence made possible by combined image analysis, clinicians can now have the documentation that they need to plan more effective procedures and thus produce better outcomes. This review focuses on the MRI anatomy of the pelvic floor from a functional point of view and from the urogynecological side of floor dysfunction (UI and POP), adopting a problem-oriented approach. The first section of this article provides the basic essential anatomical information about the pelvic floor and briefly reviews the pathophysiology and clinical features of SUI and POP. The second portion details the vital role of the radiologist in obtaining accurate images for the clinician to use in planning reconstructive surgery. In addition, it includes case examples, illustrating how to report MRI findings systematically and comprehensively on both the static and dynamic images, using a recently developed integrated MRI analytical approach from a purely functional point of view that may enhance radiologists' interaction with clinicians and bridges the gap between radiology and surgery.

Key words: Pelvic floor MRI—Pelvic floor dysfunction—Pelvic organ prolapse—Individualized treatment—Image correlation

The term *pelvic floor* refers collectively to the pelvic diaphragm, the sphincter mechanism of the lower urinary tract, the upper and lower vaginal supports, and the internal and external anal sphincters [1]. *Pelvic floor dysfunction* (PFD) is a term applied to a wide variety of clinical conditions, including urinary incontinence (UI), pelvic organ prolapse (POP), defecatory dysfunction, sensory and emptying abnormalities of the lower urinary tract, sexual dysfunction, and several chronic pain syndromes. The first three are the most common clinical conditions [2].

Each year, PFD affects between 300,000 and 400,000 American women so severely that they require surgery, and ~30% of the procedures performed are reoperations [3, 4]. In a recent study, DeLancey [3] stated that the commonness of the need for reoperation indicates that better treatments are necessary; however, he maintained that such improvement will be possible only if research clarifies the causative mechanisms and the reasons that surgery fails. In a comprehensive review, Black and Downs [5] documented the poor quality of the available data on surgical treatment of UI and concluded that

Correspondence to: Rania Farouk El Sayed; *email:* rania729@internetegypt.com

"recommendations as to the best clinical practice cannot be based on scientific evidence." In view of these data, clinicians have emphasized the desperate need for specific tests that can detect the specific anatomical defect responsible for PFD in each patient so that truly corrective treatment can be planned. DeLancey [3] predicted that with the development of such tests, the cure rate would be 100%.

Because PFD is common, clinicians have long wanted better data on which to base treatment. The usual tests and evaluation methods often do not produce satisfactory outcomes, resulting in high failure rates for surgical procedures and thus dysfunction recurrence. Recently, a new magnetic resonance imaging (MRI) analytical approach was devised that integrates data provided by both static and dynamic (cine) images, making it possible for clinicians to more accurately diagnose the underlying defects to tailor treatment to the needs of each patient [6]. Because of the promising evidence that MRI can play a role in more accurately guiding the choice of surgical technique in 41.6%–75% of patients with different spectra of PFD [7–9], my group did further study on the analysis of static and dynamic magnetic resonance images to develop a correlative analytical approach to meet clinicians' need for this specific test. This approach provides the necessary scientific evidence on which best clinical practice can be based, and the reporting system used for analysis provides an aid for accurately planning reconstructive surgery and hence may contribute to reducing the risk of surgical failure, dysfunction recurrence, and reoperation.

This review focuses on the MRI anatomy of the pelvic floor from a purely functional point of view and from the urogynecological side of floor dysfunction (UI and POP), adopting a problem-oriented approach. In this context and for didactic reasons, the first section of this article provides the basic essential anatomical information about the pelvic floor and briefly reviews the pathophysiology and clinical features of stress urinary incontinence (SUI) and POP.

The second portion details the vital role of the radiologist in obtaining accurate images for the clinician to use in planning reconstructive surgery that can help provide the best possible outcomes for their patients. In particular, the section explains how a recently developed integrated MRI analytical approach can be a crucial tool in decision making.

Because this article is problem oriented, it includes case examples, illustrating how to report MRI findings systematically and comprehensively on both the static and dynamic images, using a recently developed integrated MRI analytical approach from a purely functional point of view that may enhance radiologists' interaction with clinicians and bridges the gap between radiology and surgery.

Basic essential anatomical considerations: the pelvic floor

The term *pelvic floor* is used broadly to include all the structures supporting the abdominal and pelvic cavity. Conceptually, pelvic floor anatomy is commonly divided into passive and active structures [10] (Fig. 1). The passive structures are (1) the pelvic bones and (2) the supportive connective tissue of the pelvis, which consists of ligaments and endopelvic fascia. The active support structures are the pelvic floor muscles, with their neurological wiring that results in sustained (tonic) and intermittent voluntary muscle contractions during activity.

These passive and active components of the pelvic floor function as an integrated multilayer system (Fig. 2). From craniad to caudad, it consists of the endopelvic fascia, the pelvic diaphragm, and the urogenital diaphragm.

- *The endopelvic fascia* includes the parametrium and the paracolpium, giving support to the uterus and upper vagina, respectively.

  The paracolpium, which attach the upper vagina to the pelvic walls, can be divided into three levels [11] (Fig. 3):

  - *Level I (suspension)* The portion of the vagina adjacent to the cervix (the cephalic 2–3 cm of the vagina) is suspended from above by the relatively long connective tissue fibers of the upper paracolpium.
  - *Level II (attachment)* In the midportion of the vagina, the paracolpium become shorter and attach the vaginal wall more directly to the arcus tendineus fascia pelvis at the lateral pelvic wall. This attachment stretches the vagina transversely between the bladder and rectum and has functional significance; the structural layer that supports the bladder (the pubocervical fascia) is composed of the anterior vaginal wall and its attachment through the endopelvic fascia to the pelvic wall.
  - *Level III (fusion)* Near the introitus, the vagina is fused laterally to the levator ani and posteriorly to the perineal body, whereas anteriorly it blends with the urethra. At this level, which corresponds to the region of the vagina that extends from the introitus to 2–3 cm above the hymenal ring, there is no intervening paracolpium between the vagina and its adjacent structures, contrary to the situation at levels I and II.

- *The pelvic diaphragm*, including the levator ani (puborectalis and iliococcygeus) and the coccygeus muscles, acts as a shelf supporting the pelvic organs.
- *The urogenital diaphragm*, the most caudal layer of the pelvic floor, is composed of connective tissue and the deep transverse peroneus muscle.

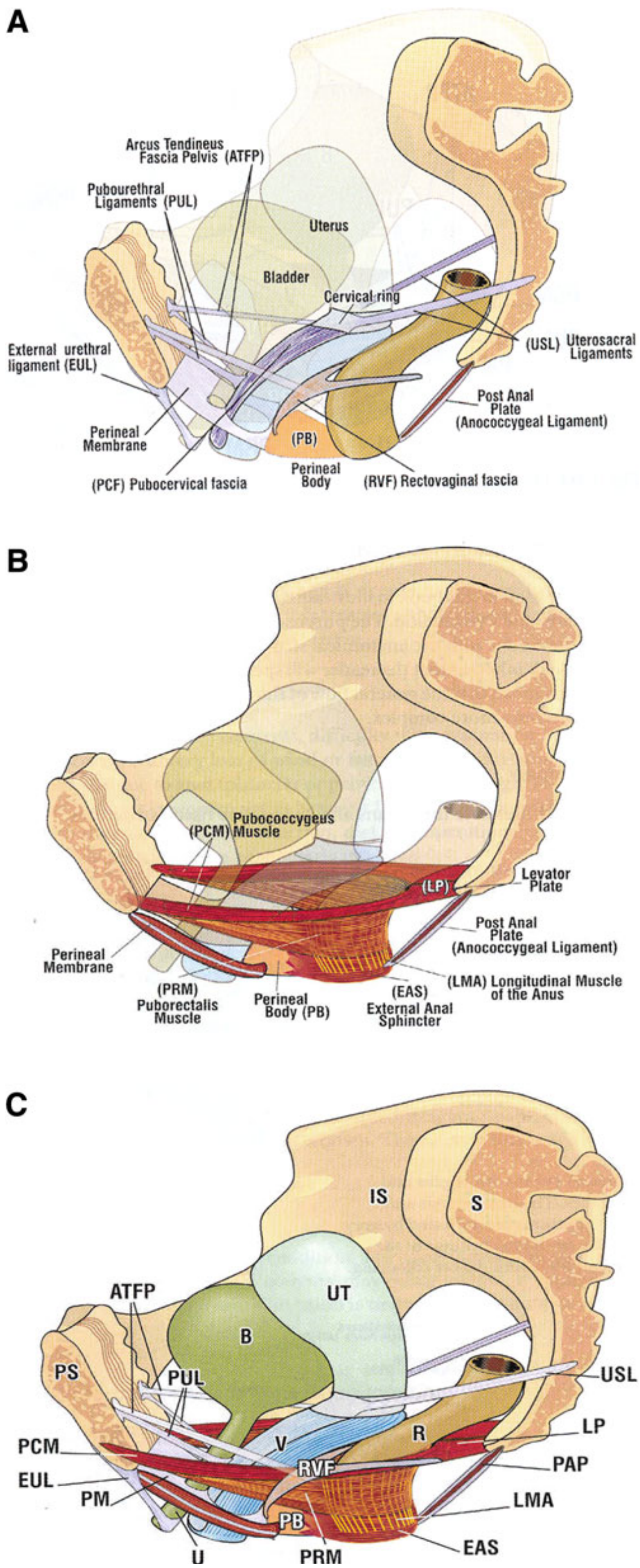

◀ **Fig. 1.** Passive and active structures of the pelvic floor: **A** Pelvis with organs and connective tissue. The ligamentous and membranous structures are indicated by shades of *gray*, and the fascial thickenings of the vagina (PCF, RVF) are *darker*. **B** Pelvis with organs and muscles (muscles are *brown* with striations). **C** The relationship of the pelvic muscles to organs, ligaments, and fascia. (Reproduced by permission from Petros [59].)

For the purpose of evaluating and describing PFD, the pelvis is divided into three compartments: an anterior compartment containing the bladder and urethra, a middle compartment containing the uterus and cervix (or the vaginal cuff in women who have undergone a hysterectomy), and a posterior compartment containing the rectum and anal canal.

Pathophysiology and clinical features of PFD

Stress UI

Definition and classification. As classified by the International Continence Society (ICS), UI of all types is defined as involuntary loss of urine that is both objectively demonstrable and socially or hygienically problematic for the patient [12, 13]. Common subtypes of UI include stress urinary incontinence (SUI), urge urinary incontinence (UUI), and mixed urinary incontinence (MUI). The symptom of SUI is involuntary leakage on effort, whereas the symptom of UUI is involuntary leakage accompanied by or immediately preceded by urgency. MUI is a combination of SUI and UUI [12]. Most reports of large community-based or general-practice epidemiologic surveys in adult women of all ages show prevalence rates for UI of 20%–50% [14, 15]. SUI is the most common type of incontinence in women, with 86% of incontinent women presenting with the symptoms of either pure (50%) or mixed (36%) forms of SUI [16].

The ICS has developed standard definitions for SUI and introduced the concept of SUI as symptom, sign, and condition. The symptom is involuntary leakage on exertion or on sneezing or coughing. The sign is observable involuntary leakage from the urethra, synchronous with effort or exertion or with sneezing or coughing. The condition of genuine (urodynamic) stress incontinence is noted during filling cystometry and is defined as involuntary leakage of urine during increased abdominal pressure, in the absence of a detrusor contraction. Most importantly, to women themselves, SUI may mean social isolation or the inability to perform physical activities without fear of leakage [12].

Pathophysiology of SUI. The precise anatomical causes of SUI remain somewhat unclear. It has been attributed to urethral hypermobility [17, 18], to unequal movement of the urethral walls [19], and to defects in the urethral supporting structures [20, 21]. Another type is intrinsic sphincter deficiency, caused by a poorly functioning urethral sphincter muscle [22].

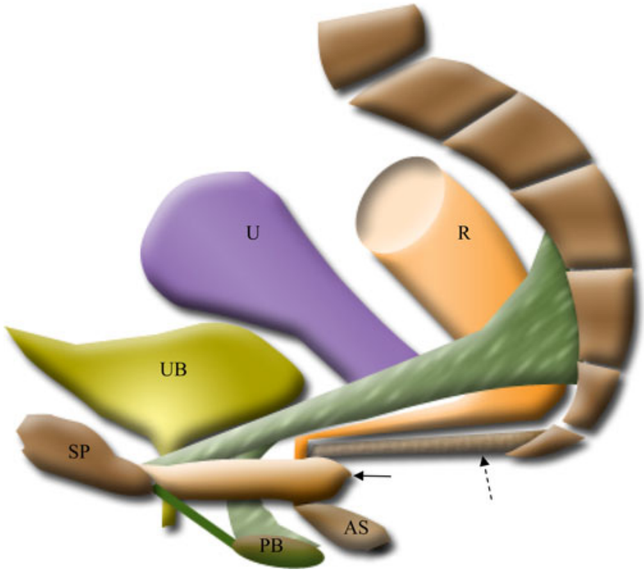

Fig. 2. Three-dimensional schematic of the components of the pelvic floor integrated into a multilayer system, from craniad to caudad, consisting of the following: (1) the endopelvic fascia, giving support to the uterus and upper vagina (*light green*), (2) the pelvic diaphragm, including the puborectalis (*solid arrow*) and iliococcygeus (*dashed arrow*), and (3) the urogenital diaphragm (*dark green*). *AS* anal sphincter complex, *PB* perineal body, *R* rectum, *SP* symphysis pubis, *U* uterus, *UB* urinary bladder. (Modified by permission from Beco and Mouchel [43].)

Clinical assessment and investigation. Clinical evaluation. Women who are being assessed for UI are asked to maintain a diary of urinary pad use for at least 3 days for each episode for data collection. They record and report pad use, UI episodes, and urinary frequency. Physical examination may include a cotton swab test to identify bladder neck hypermobility [23] and a full bladder cough stress test to elicit the sign of SUI. In addition, these women are tested for urinary tract infection [24].

Urodynamic studies. Several urodynamic studies are conducted, including multichannel cystometry and Valsalva leak point pressure.

Multichannel cystometry

- Differentiates SUI from UUI
- Indicates UUI through an increase in intravesical pressure, which is consistent with a bladder detrusor muscle contraction and implies detrusor instability or UUI [24, 25].

Valsalva leak point pressure

- Can identify SUI that is caused by intrinsic urethral sphincter deficiency (Fig. 4)

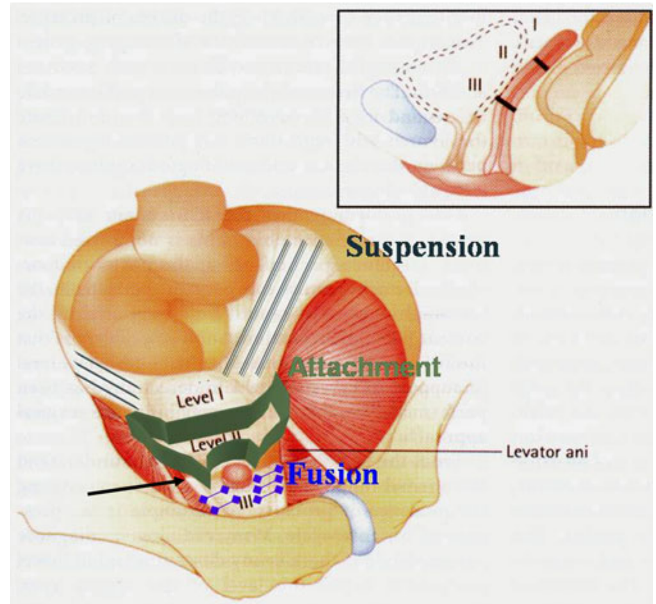

Fig. 3. Levels of vaginal support after hysterectomy. In level I (suspension), the paracolpium suspends the vagina from the lateral pelvic walls. Fibers of level I extend both vertically and posteriorly toward the sacrum. In level II (attachment), the vagina is attached to the arcus tendineus fasciae pelvis (*solid arrow*) and the superior fascia of levator ani. In level III (fusion), the vagina, near the introitus, is fused laterally to the levator ani. (Modified by permission from Hale et al. [60].)

- At different volume intervals during filling cystometry, the patient is asked to strain until leakage is observed and the pressure within the bladder is measured. There is a consensus that a Valsalva leak point pressure of <60 cm H_2O at a volume of 150 filling correlates with intrinsic sphincter deficiency [25, 26].

Diagnostic problems. Urodynamics (especially medium-fill cystometry) have been generally accepted as the cornerstone of differentiation of SUI from UUI. However, the correlation between urodynamic findings and UI symptoms is generally poor, particularly in patients with symptoms of MUI. Therefore, the reliability of cystometry has been questioned recently [27]. It has been suggested that it would be more appropriate to consider the patient's symptoms and physical signs in clinical decision making. Nonetheless, the accuracy of symptom-based diagnosis has been disappointing, and there have been attempts to improve both its objectivity and reliability [27]. MRI can provide objective documentation of anatomical and structural abnormalities.

Pelvic organ prolapse

Definitions and classification. The term *prolapse* is commonly used to describe any degree of downward pelvic organ movement, but by definition, it refers to complete

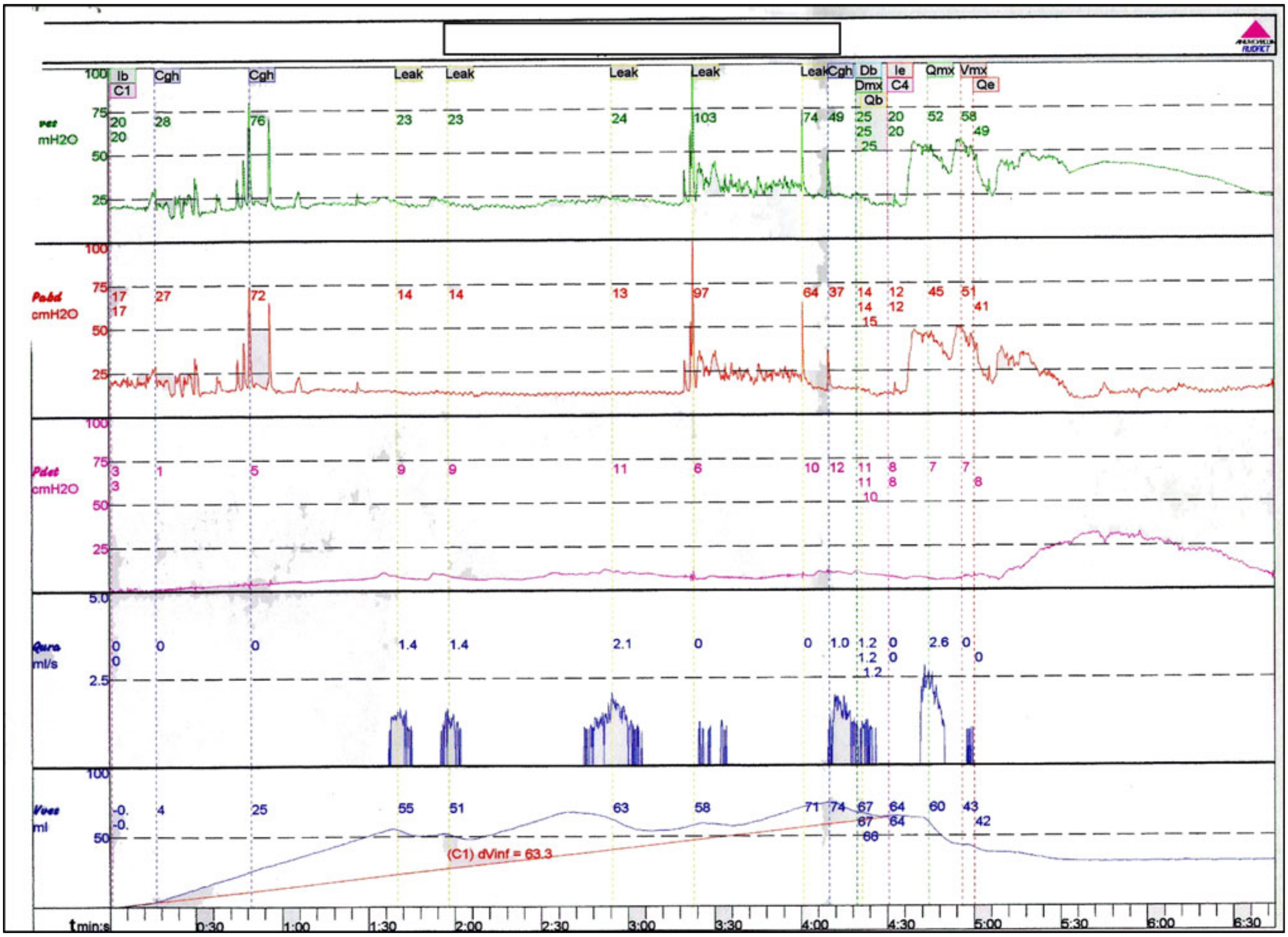

Fig. 4. Multichannel cystometry in patient with SUI due to intrinsic urethral sphincter deficiency. The Valsalva leak point pressure was <60 cm H_2O, suggestive of intrinsic sphincter deficiency. *Pabd* abdominal pressure measured by a catheter within the rectum or vagina, *Pves* bladder pressure measured with a catheter in the bladder, *Pdet* true detrusor pressure by the bladder, which is calculated by the formula Pdet = Pves − Pabd.

organ eversion. This latter definition is usually used in describing the posterior compartment, where a distinction is more commonly made between true rectal prolapse (invagination and eversion of the rectum) and rectal descent without eversion due to pelvic floor weakness [28]. The term *prolapse* is used here in its more general sense to remain consistent with prior publications.

POP includes anterior vaginal prolapse (cystocele), apical or uterine prolapse, and posterior vaginal prolapse, which includes enterocele, rectocele, and perineal descent but does not include rectal prolapse.

Pathophysiology. POP has been attributed both to damage to the levator ani muscle [29] (where weakness of the levator ani may cause widening of the levator hiatus and descent of the central portion of the pelvic diaphragm) and to an endopelvic fascial defect [30]. However, DeLancey [31, 32] described the interaction between pelvic floor muscles and endopelvic fascia and maintained that it is not possible to determine which is responsible for prolapse—damage to muscle or damage to fascia—because these two aspects of pelvic support are intimately interdependent.

Clinical assessment and investigation. POP—especially uterine prolapse—is more commonly diagnosed and staged by physical examination. In 1996, the American Urogynecological Society, the Society of Gynecologic Surgeons, and the ICS adopted a system for the evaluation of POP: Pelvic Organ Prolapse Quantitation, which identifies 9 points for measurement and prolapse staging (Table 1) [33].

Cystoceles. It can be classified by grade according to the degree of bladder descent or by anatomical defect (central, lateral, or combination). Most grade 1 and 2

Table 1. POP quantitation

Description	Stage
No prolapse is demonstrated	0
The most distal portion of the prolapse is >1 cm above the level of the hymen	I
The most distal portion of the prolapse is ≤1 cm proximal to or distal to the plane of the hymen	II
The most distal portion of the prolapse is >1 cm below the plane of the hymen but protrudes no further than 2 cm less than the total vaginal length in centimeters	II
Essentially complete eversion of the total length of the lower genital tract is demonstrated	IV

cystoceles are asymptomatic but can be associated with SUI. Marked cystocele is commonly symptomatic and can be associated with the following:

- Vaginal bulging
- Dyspareunia
- Urinary tract infection, obstructive voiding symptoms, and urinary retention.

Uterine prolapse. Mild uterine prolapse is usually asymptomatic, but higher grades can present as follows [34]:

- A vaginal mass, dyspareunia, and stretching of the uterosacral ligaments, which may lead to low back pain
- Urinary retention and obstructive uropathy due to ureteral obstruction
- Difficulty in defecating (experienced by one-third of patients with prolapse).

Enteroceles. Simple enterocele exists when there is no associated vault prolapse and the cuff of the vagina is well supported. Complex enterocele is associated with vault prolapse and tends to coexist with other forms of prolapse of the anterior or posterior vaginal wall. Symptomatic enterocele may cause

- Vaginal pressure, dyspareunia, a dragging sensation in the pelvis, and pelvic pressure
- Stretching of the mesentery with straining, which can cause pain in the lower abdomen or back [35]
- Severe constipation, a feeling of incomplete evacuation, or symptoms of bowel obstruction [36].

Diagnostic problems. Difficulties in clinical assessment and treatment of patients with POP are usually encountered and include the following:

- *Difficulty in differentiating a high-grade cystocele from an enterocele, a vaginal vault prolapse, or a high rectocele by physical examination* [28, 37, 38]. A high-grade cystocele may mask SUI [39]; anti-incontinence procedures usually result in improvement through restoration of the normal pelvic floor anatomy. In addition, repairing a cystocele without attention to the rest of the pelvic floor may predispose the patient to an increased incidence of enterocele, rectocele, or uterine prolapse after the operation [9, 40].
- *Difficulty in detecting enteroceles on physical examination because of vaginal overcrowding* [28]. In a number of patients, clinical findings may not correlate with symptoms, as these patients may have a degree of descent sufficient to cause symptoms, but because they have a deep pelvis, the extent of the prolapse is not appreciable on clinical examination [41].

Recommendations for clinical assessment of PFD

In view of the diagnostic problems encountered in SUI and POP, three-axis perineal evaluation (TAPE) is recommended in the assessment of a patient presenting with PFD, even if the main symptom is apparently related to one of the three pelvic compartments. Combining TAPE with the newly developed MRI analytical approach puts a complete assessment of the patient, both clinically and radiologically, within reach of both radiologists and clinicians.

Anatomically, each organ system in the pelvic floor—urinary, genital, and intestinal—traverses the pelvis and exits through its own orifice. Thus, these systems are intricately related in function and structural support [42]. This has been proven by findings that among patients with PFD, 95% have abnormalities in all the three pelvic compartments, although patients may present with symptoms that involve only one compartment [1]. Therefore, disorders of each of these components should be evaluated in light of their impact on the function of the surrounding structures and the functional anatomy of the pelvic floor [42]. Hence, physicians treating women with PFD should adopt a global approach, taking into consideration all the three pelvic compartments, and must clearly understand the anatomy of the pelvis and the associated urinary, genital, and anorectal abnormalities.

Beco and Mouchel [43] have defined a TAPE approach, which they call perineology (Fig. 5). This approach is the result of the fusion between the disciplines of urogynecology and coloproctology. The aim of perineology is anatomical restoration with respect to biomechanics and physiology, so that each defect must be corrected without inducing trouble on other levels. Therefore, if, for example, reconstructive surgery is to be performed for patients with POP, then correction of all the anatomical defects should be achieved to prevent subsequent recurrence or exaggeration of other compartment defects. This calls for noninvasive preoperative and postoperative imaging methods that can depict the

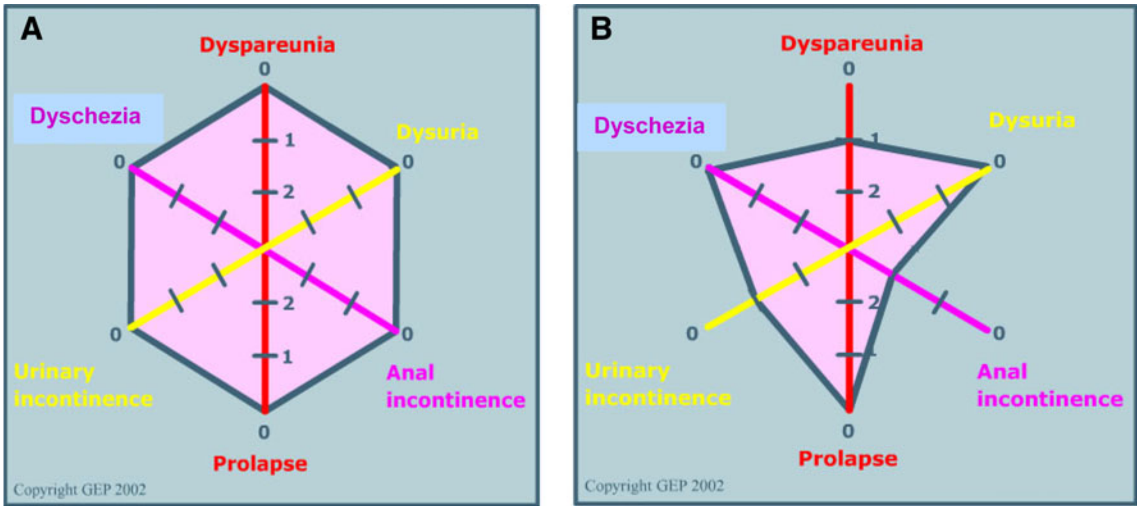

Fig. 5. **A** TAPE is hexagonal and has three axes, each of which represents a continuum of problems, from excess to deficiency. The gynecologic axis is in *red*; at the excess end is dyspareunia, and at the deficiency end is prolapse. The urologic axis is in *yellow*; on the excess end is dysuria, and on the deficiency end is urinary incontinence. The coloproctologic axis is in *pink*; on the excess end is dyschezia, and on the deficiency end is anal incontinence. For each axis, there are three levels of severity: 0 = no problem, 1 = mild problem, 2 = severe problem. **B** TAPE in a patient with problems on all three axes: mild dyspareunia, severe anal incontinence, and mild UI. If the gynecologist does not ask the right questions, the patient will have to live with her problems for many years. (Modified by permission from Beco and Mouchel [43].)

three pelvic compartments simultaneously. MRI is ideal for this purpose [7].

MRI and PFD

MRI has been effectively used to evaluate PFD, with very good reported sensitivity, specificity, and positive predictive value. The modality relies on (a) static sequences with a high spatial resolution to delineate the passive and active elements of the pelvic organ support system and on (b) fast imaging dynamic (cine) sequences during rest and straining for detection of functional abnormality. However, because each of those passive or active structural components plays a role either in continence (urinary and fecal) or in preventing POP, the involvement of these elements in the pathogenesis of various dysfunctions cannot be fully understood with the current classification system. To gain insight in the underlying pathology so that radiologists can accurately define the structural defect, we must adopt a new, more function-based classification of the pelvic organ support system that groups all of the structures that contribute to the same function under one system. Therefore, all of the structures that maintain urinary continence can be grouped under the term *urethral support system*, the supporting elements that prevent prolapse can be grouped under the term *vaginal support system*, and the anal sphincter complex is the main component responsible for anal continence.

Our recently described MRI analytical approach to define the predominant defects of the pelvic support system is described in the following section, which also explains why this approach was developed and how to apply it [6]. To make it easy for radiologists to use this approach and to increase surgeons' comprehension of the overall findings, we created an MRI reporting form in which all data are presented in schematic form (Table 2). A diagnostic algorithm (Fig. 6) can be used to help tailor imaging according to the patient's symptoms and the clinical findings [44].

Imaging protocol

There is no standardized protocol for MRI of patients with PFD. However, the key element of any protocol is to image the patient during maximal strain or rectal evacuation in one or more planes [28]. The following is an example of the protocol used in our institution [6]. MRI is performed with the patient supine in a 1.5-T MRI unit (Gyroscan PowerTrak 6000, Philips Medical Systems, Best, Netherlands) using a pelvic phased-array coil.

- Patient preparation:
  - No oral or intravenous contrast agent is administered.
  - All the patients undergo a cleansing rectal enema (using warm water) the night before the MRI examination and are asked to void 2 h before the examination.

Table 2. MRI report

Dynamic Magnetic Imaging Findings

Location of Prolapse	Type of Prolapse	Grade
Anterior compartment	Bladder neck descent	____________________
	Bladder base descent	____________________
Middle compartment	Uterine descent	____________________
	Enterocele/peritoneocele	____________________
Posterior compartment	Anorectal junction descent	____________________
	Rectocele	____________________

Measurement of Supporting Structures	Value	Mean and SD[a]
H-line	____________________	5.8 ± –0.5 cm
M-line	____________________	1.3 ± 0.5 cm
Levator plate angle (LPA)	____________________	11.7° ± 4.8°
Width of levator hiatus (WLH)	____________________	4.5 ± 0.7 cm
Iliococcygeus angle (ILc A)	____________________	33.4° ± 8.2°

Static Magnetic Resonance Imaging Findings

Defects in the Pelvic Organ Support System	Structure	Type of Injury/Weakness	Side of Injury
Urethral supporting structures	Ligament(s)	__________________	__________________
	Fascia level III	__________________	__________________
	Puborectalis	__________________	__________________
Vaginal supporting structures	Vaginal fascia level I and II	__________________	__________________
	Iliococcygeus	__________________	__________________

Anal Sphincter Complex	Muscle Affected	Type of Injury	Site and Level of Injury
	External anal sphincter	__________________	__________________
	Internal anal sphincter	__________________	__________________

Correlation Between Static and Dynamic Magnetic Resonance Imaging Findings

Predominant Defect(s)	Stress Urinary Incontinence	Pelvic Organ Prolapse	Anal Incontinence
Ligaments	____________________		
Fascia	____________________	____________________	
Muscles (Puborectalis, Iliococcygeus)	____________________	____________________	____________________
Anal sphincter complex	____________________	____________________	____________________

[a] Data from El Sayed et al. [6]

– Using 60-mL syringes, 90–120 mL of ultrasonographic gel (Aquasonic, Parker Laboratories, Fairfield, NJ) is placed into the rectum.

- Imaging parameters for static images:

– Static images of the pelvis are acquired in three planes using T_2-weighted turbo spin-echo (TSE) sequences [repetition time ms/echo time ms (TR/TE) 5000/132, field of view (FOV) 240–260 mm, slice thickness 5 mm, gap 0.7 mm, number of signals acquired 2, flip angle 90°, matrix 512 × 512, acquisition time 3.12 min for each sequence].

– In addition, T_2-weighted balanced fast field echo (BFFE) images (9.0/4.0, field of view 220 mm, section

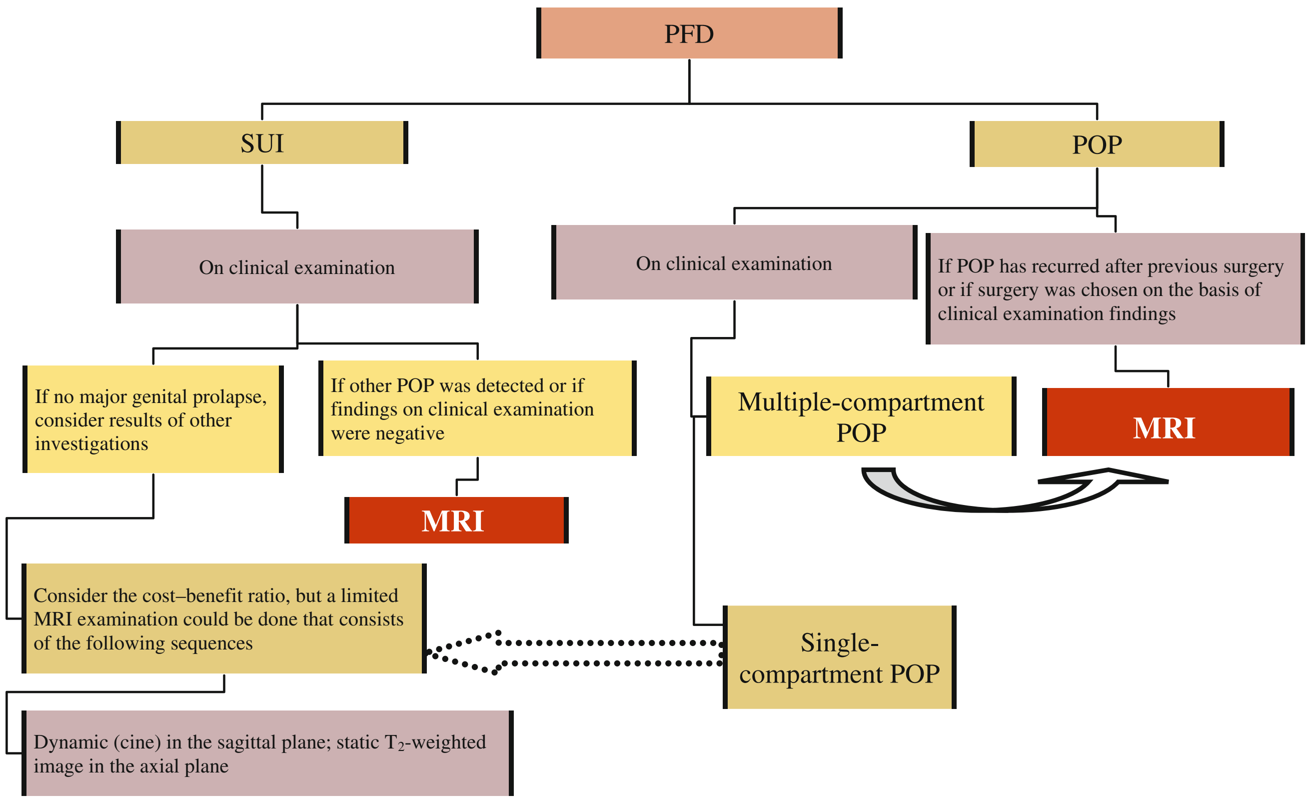

Fig. 6. A diagnostic algorithm for MRI of patients with pelvic floor dysfunction. *PFD* pelvic floor dysfunction, *POP* pelvic organ prolapse, *SUI* stress urinary incontinence.

thickness 3 mm, number of signals acquired 8, flip angle 45°, matrix 512 × 512, acquisition time 2.12 min) of the anal sphincter complex are obtained if the patient is complaining from anal incontinence. In this sequence, section orientation is parallel and perpendicular to the plane of the anal canal.

- Imaging parameters for dynamic (cine) images:

– Dynamic sequences are performed in the sagittal, axial, and coronal planes, using a BFFE sequence (TR/TE 5.0/1.6 ms, FOV 300 mm, slice thickness 6–7 mm, gap 0.7 mm).
– In each plane, 5 slices during 6 phases are acquired; each phase take 10 s. These six phases are acquired (1) with the patient at rest, (2) during contraction of the pelvic floor (the patient is instructed to squeeze the buttocks as if trying to prevent the escape of urine), (3) during mild straining, (4) during moderate straining, (5) during maximum straining, and (6) during a repeated maximum straining sequence to ensure a maximal Valsalva maneuver (the patient is instructed to bear down as much as she can, as though she is constipated and trying to defecate).

Analysis of static magnetic resonance images

Analysis of static images is based on thorough examination of the pelvic organ supporting elements and characterizations of the defects in each of its components: the urethral supporting system, the vaginal supporting system, and the anal sphincter complex.

The urethral supporting system. Scrutiny of the urethral support system involves imaging of the urethral ligaments, endopelvic fascia (level III fascial support), and the puborectalis muscle (Fig. 7).

- Urethral ligaments:

– *MRI of normal urethral ligaments* Meticulous cadaveric dissection identified ventral and dorsal urethral ligaments on axial T_2-weighted TSE sequences. The ventral urethral ligaments included the pubourethral ligaments, which were found to consist of three separate components running anteroposteriorly from the bladder neck to the pubic bone [45], the periurethral ligament, and the paraurethral ligaments [46].

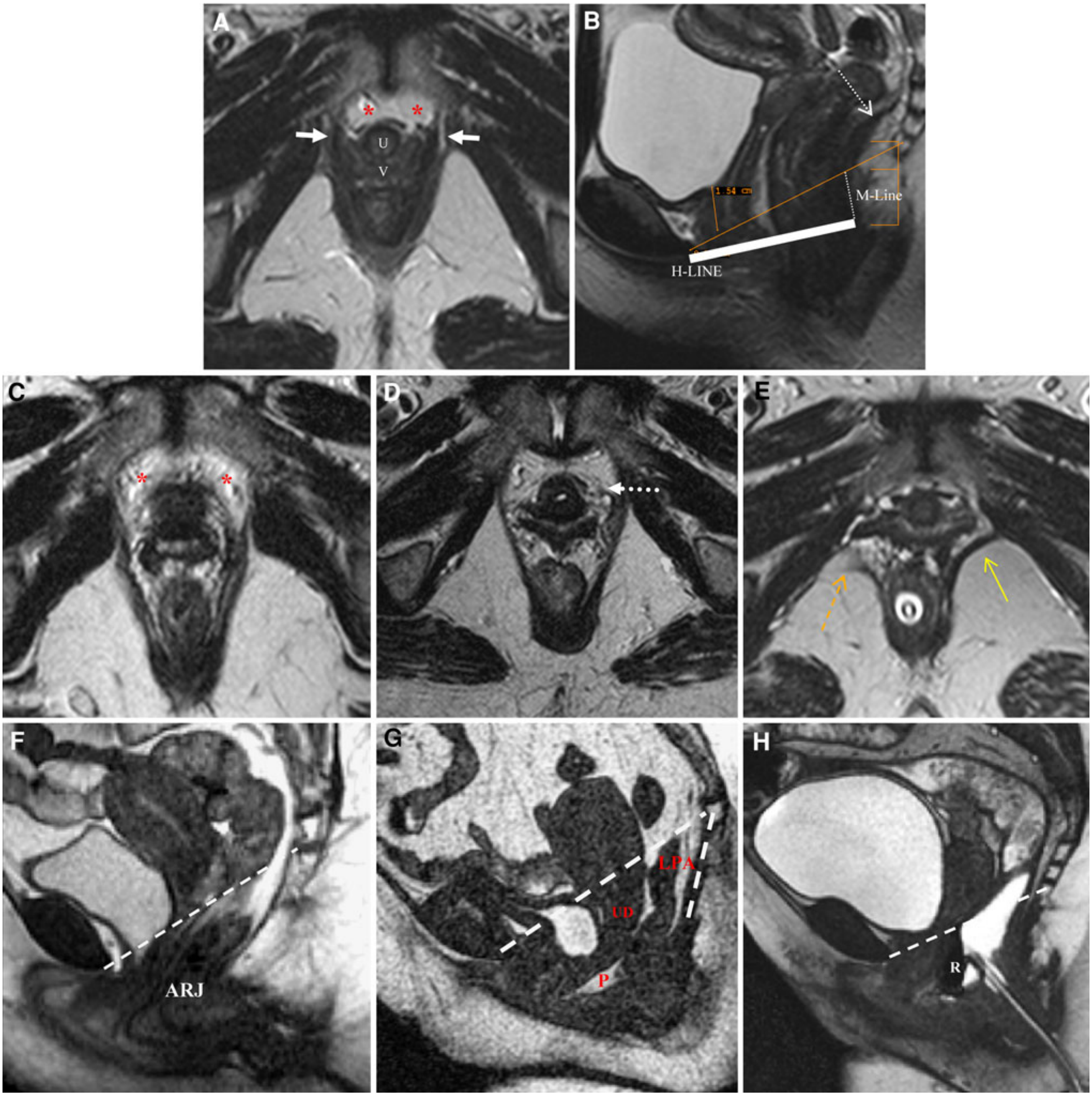

– Dorsal to the urethra, a sling-like ligament, the "suburethral ligament," was identified. This ligament had a distinct plane of cleavage from the anterior vaginal wall. To the best of our knowledge, this ligament had not been reported before [45]. The MRI findings in volunteers correlated with the MRI and gross anatomical findings in cadavers. The proximal pubourethral, periurethral, paraurethral, and suburethral ligaments had visibility scores of 3 (moderately visible) or 4 (easily visible) on MRI in 47%, 65%, 47%, and 53% of volunteers, respectively [45].

– *MRI of urethral ligament abnormalities* On images obtained in the axial plane, abnormalities are classified as follows:

  - Distortion, when internal architectural changes with waviness of the ligaments are seen
  - Defects, defined by discontinuity of the ligament with visualization of the torn parts [20, 46]

- *Level III fascial defect* This is assessed at the level of urethra and bladder neck. It is recognizable by the drooping mustache sign, which is caused by the fat in

◀ **Fig. 7.** Normal urethral supporting system and types of anatomical defects. **A**, **B** Axial and sagittal magnetic resonance images from a 27-year-old healthy, continent volunteer. **A** Static T_2-weighted TSE image (repetition time ms/echo time ms [TR/TE] 5000/132) at the level of the proximal urethra (U) shows normal level III endopelvic fascial support. *Arrows* point to the attachment of the puborectalis slings to the symphysis pubis, *space of Retzius, *V* vagina. **B** Dynamic sagittal BFFE MR images (TR/TE 9/4) obtained at maximum straining; there is no bladder base or pelvic organ descent below the pubococcygeal line (PCL) and no excessive levator plate angulation (*dashed arrow*) in relation to the PCL. The H- and M-line are illustrated. **C**–**E** Static axial T_2-weighted TES images at the same level as **A** illustrating different patterns of defects in 3 patients who reported SUI. **C** **Level III facial defect with the typical magnetic resonance appearance of the drooping mustache sign. **D** Urethral ligament abnormalities: there is deformation of the peri-urethral ligaments on the left side (*dashed arrow*), with discontinuity of the ligament on the right side. **E** Muscle defect: compared to the left puborectalis muscle sling, there is discontinuity of the muscle fibers on the right side (*dashed arrow*). **F**–**H** The corresponding dynamic sagittal BFFE (TR/TE 9/4) images obtained at maximum straining of the same patients as in **C**–**E**. The images show minimal (**F**), moderate (**G**), and no (**H**) descent of the bladder neck and base. Combined analysis of static and dynamic images confirmed that although the 3 patients clinically have the same symptoms, there is a different underlying structural abnormality in each requiring an individually tailored surgical technique. Other associated findings include the following: **F** anorectal junction descent (ARJ) and a levator plate angle (LPA) of 30°, **G** uterine descent (UD), peritoneocele (P), and an LPA of 59°, **H** a small anterior rectocele (R) and an LPA of 55°.

the prevesical space against the bilateral sagging of the detached lower third of the anterior vaginal wall from the arcus tendineus fascia pelvis [47].

- *Puborectalis muscle defect* This is recognizable by disruption of the normal symmetrical appearance of the muscle sling or of its attachment to the symphysis pubis [48].

The vaginal supporting system. Vaginal supporting structures include level I endopelvic fascia, at the level of the funds of the bladder; level II endopelvic fascia, at the trigone or bladder base; and the iliococcygeus muscle (Figs. 8, 9).

- *Level I and II endopelvic fascial defect* In the axial plane, a paravaginal defect in the fascia is visualized as sagging of the fluid-filled posterior urinary bladder wall, caused by the detachment of the vaginal supporting fascia from the lateral pelvic wall, known as the saddlebags sign [47]. A central defect is also indicated by sagging of the central part of the urinary bladder posterior wall [6].
- *Iliococcygeus muscle* In the coronal plane, the iliococcygeus muscle is assessed for loss of the normal symmetrical appearance of its muscle slings or defect and/or disruption of its attachment to the obturator internus muscle.

The anal sphincter complex. On axial T_2-weighted BFFE images the consecutive layers of the anal sphincter from the lumen outward include the innermost high-signal-intensity layer (the combined mucosa and submucosa), the low-signal-intensity layer (the submucosal smooth muscle), the internal anal sphincter (of homogenous intermediate to high-signal intensity), and the deep external anal sphincter (of low to intermediate signal intensity) [6].

- *Anal sphincter lesions are classified according to* the muscle injured (the internal or external anal sphincter or the puborectalis muscle) and according to lesion type (defect and/or scarring). A sphincteric defect is defined as discontinuity of the muscle ring; scarring is defined as a low-signal intensity deformation of the normal pattern of the muscle layer.

Analysis of dynamic magnetic resonance images

POP is best evaluated on midsagittal true fast imaging dynamic evacuation sequences and sagittal, axial, and coronal images during maximum straining, when pelvic organ descent should be greatest. As with cystoproctography, a point of reference for rest and stress measurements is required to be able to determine the presence and extent of POP [6, 28].

Several reference points and lines for measuring and staging POP on MRI have been proposed. The two most commonly used lines are a line connecting the inferior aspect of the pubic symphysis to the last coccygeal joint, the pubococcygeal line (PCL); and a line extending caudally along the long axis of the symphysis pubis, the mid-pubic line (MPL) [41, 49–51].

Once the MRI reference line is chosen, staging of POP in all the three compartments can be performed by measuring the perpendicular distance from the anatomical reference point in each compartment to the reference line. In the anterior compartment, the reference point is the most posterior and inferior aspect of the bladder base. In the apical compartment, the reference point is the anterior cervical lip, or the postero-superior vaginal apex if the patient has undergone hysterectomy. In the posterior compartment, the anterior aspect of the anorectal junction serves as the point of Ref. [28].

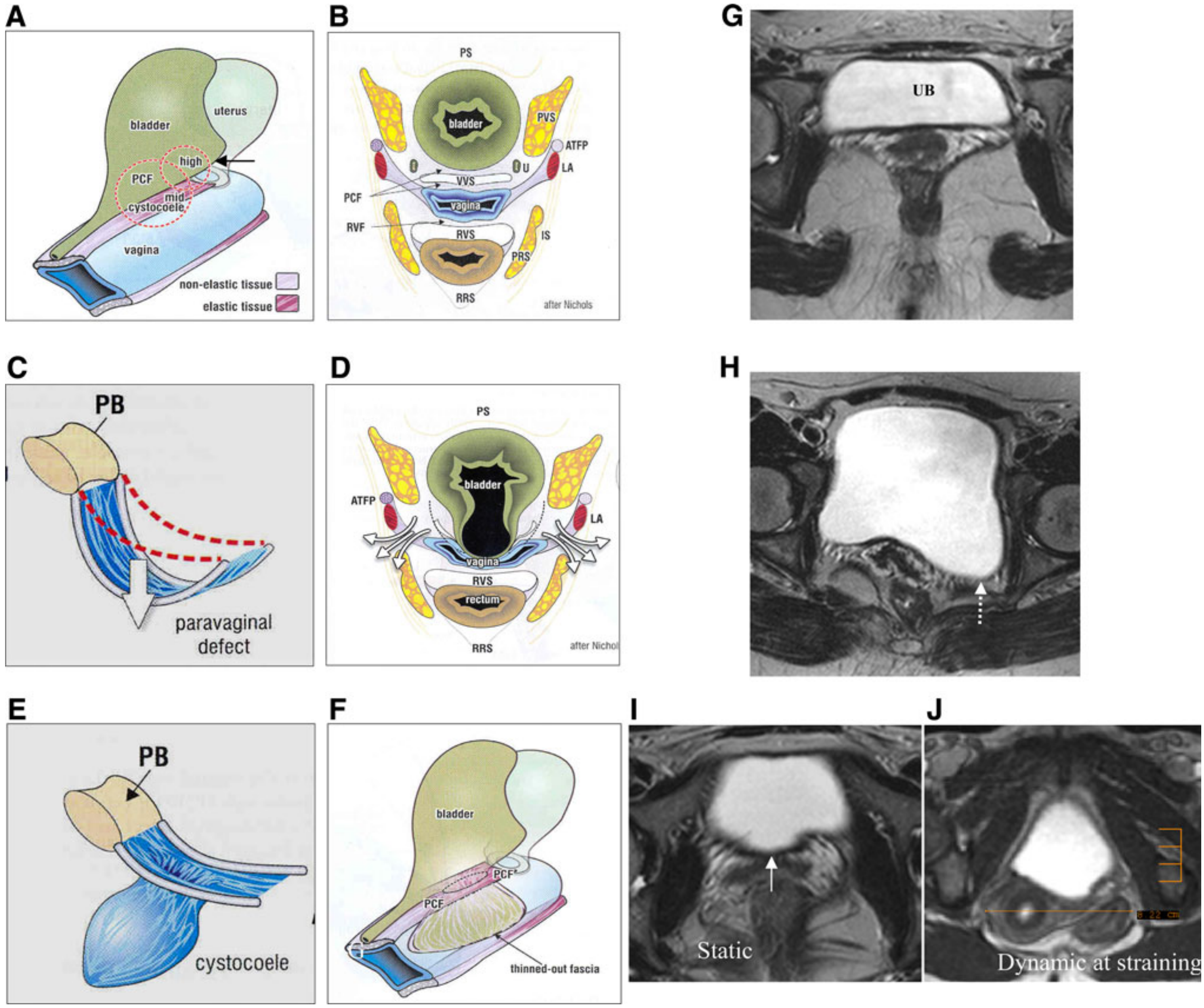

Fig. 8. A–**F** Schematic diagrams and **G**–**I** axial T_2-weighted TSE image magnetic resonance images (5000/132) at levels I and II endopelvic fascial support illustrating the structural difference between lateral (paravaginal) and midline (cystocele) defects, and how these are visualized on MRI, differentiating the type and site of each defect. **A**, **B** The pubocervical fascia (PCF) is intact, supporting the urinary bladder and maintaining a straight posterior bladder wall (*arrow* in **A**). This is what is also seen in **G**: the straight posterior wall of the urine-filled urinary bladder (UB). **C**, **D** The site of breaks in the PCF in paravaginal defect. On the magnetic resonance image, a defect in the fascia is not apparent. However, its effect on the urinary bladder is apparent where its adjacent wall (the posterior) creeps inside the defect, creating the saddlebags sign as shown in **H**, which is more severe on the left side (*arrow*), indicating that the size of defect is larger and hence the bladder wall sags deeper. **E**, **F** Thinning of the PCF causes prolapse of the bladder base, seen in the three-dimensional sagittal view **F**. **I** Axial magnetic images show changes in the site of the sagging posterior urinary bladder wall "central" (*arrow*). **J** The changes are even more apparent during straining. (**A**–**F** reproduced with permission from Petros [61].)

The following are the criteria measured during maximum straining that are used in the integrated analytical approach used in my institution [6].

Sagittal plane. In the sagittal plane, the PCL is used as the reference line. It extends from the inferior border of the symphysis pubis anteriorly to the tip of the coccyx posteriorly [7].

The descent of the bladder neck, bladder base, uterus, and anorectal junction, measured perpendicularly below the PCL, is recorded [52]. Prolapse severity can be easily graded according to the "rule of three": prolapse of an organ below the PCL by ≤3 cm is mild, by 3–6 cm is moderate, and by >6 cm is severe [49, 53].

SUI is recorded when loss of urine through the urethra is visualized at maximum straining. However, the

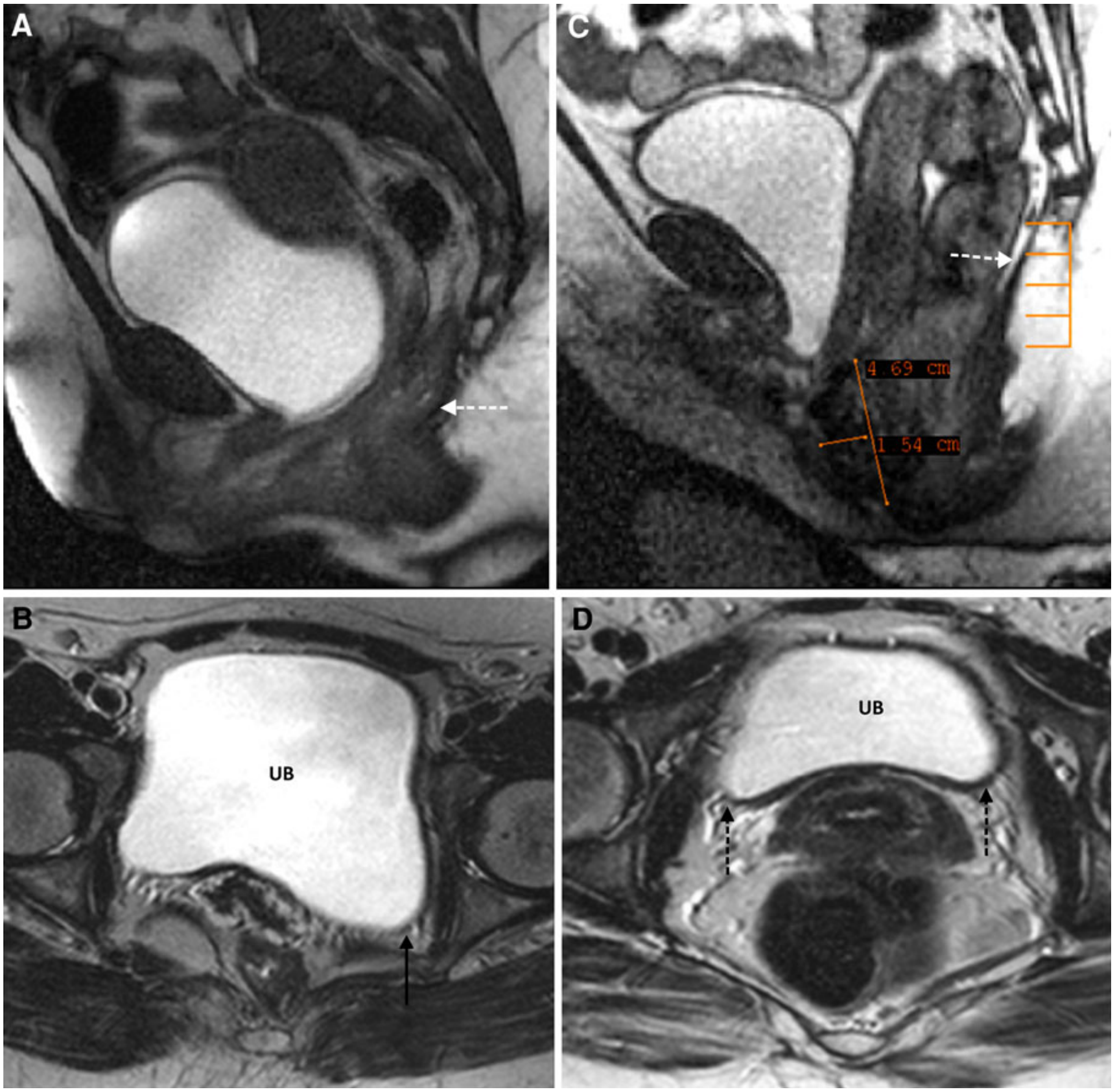

Fig. 9. Correlation between static and dynamic magnetic resonance images to specify the predominant underlying defect in 2 patients with POP. **A**, **C** Dynamic sagittal BFFE (TR/T 9/4) images, showing cystoceles of different grades, sagging of the levator plate (*dashed arrows*) that is more advanced in **C** with uterine descent (UD), and a small rectocele (R). It is not possible from these midline images to see the specific underlying structural defect. **B**, **D** The corresponding axial T_2-weighted TSE images (5000/132) at level II endopelvic fascial support. **B** Bilateral asymmetrical level II paravaginal fascial defects that is more severe on the left side (*arrow*), indicated by the sagging posterior wall of the urine-filled urinary bladder (UB). **D** Mild bilateral symmetrical fascial defects (*dashed arrows*). Combined analysis of static and dynamic magnetic resonance images and correlation between findings indicated that in **A** and **B**, POP is due to the more advanced fascial defects compared with the moderate sagging of the levator plate, whereas in **C** and **D**, the more advanced degree of muscle weakness compared with the fascial status indicates that muscle weakness is the main factor responsible for POP.

absence of urine loss during MRI does not preclude the patient experiencing symptoms.

Other measurements in the sagittal plane during maximum straining include (Fig. 7)

- The H-line, which extends from the inferior aspect of the pubic symphysis to the anorectal junction
- The M-line, dropped as perpendicular line from the PCL to the posterior aspect of the H-line [38]
- The levator plate angle, enclosed between the levator pate and the PCL [53].

Axial and coronal planes. In the axial planes (Fig. 10D, E), the width of the levator hiatus is enclosed between the puborectalis muscle slings [36]. It is measured at the most inferior point of the symphysis pubis. The transverse

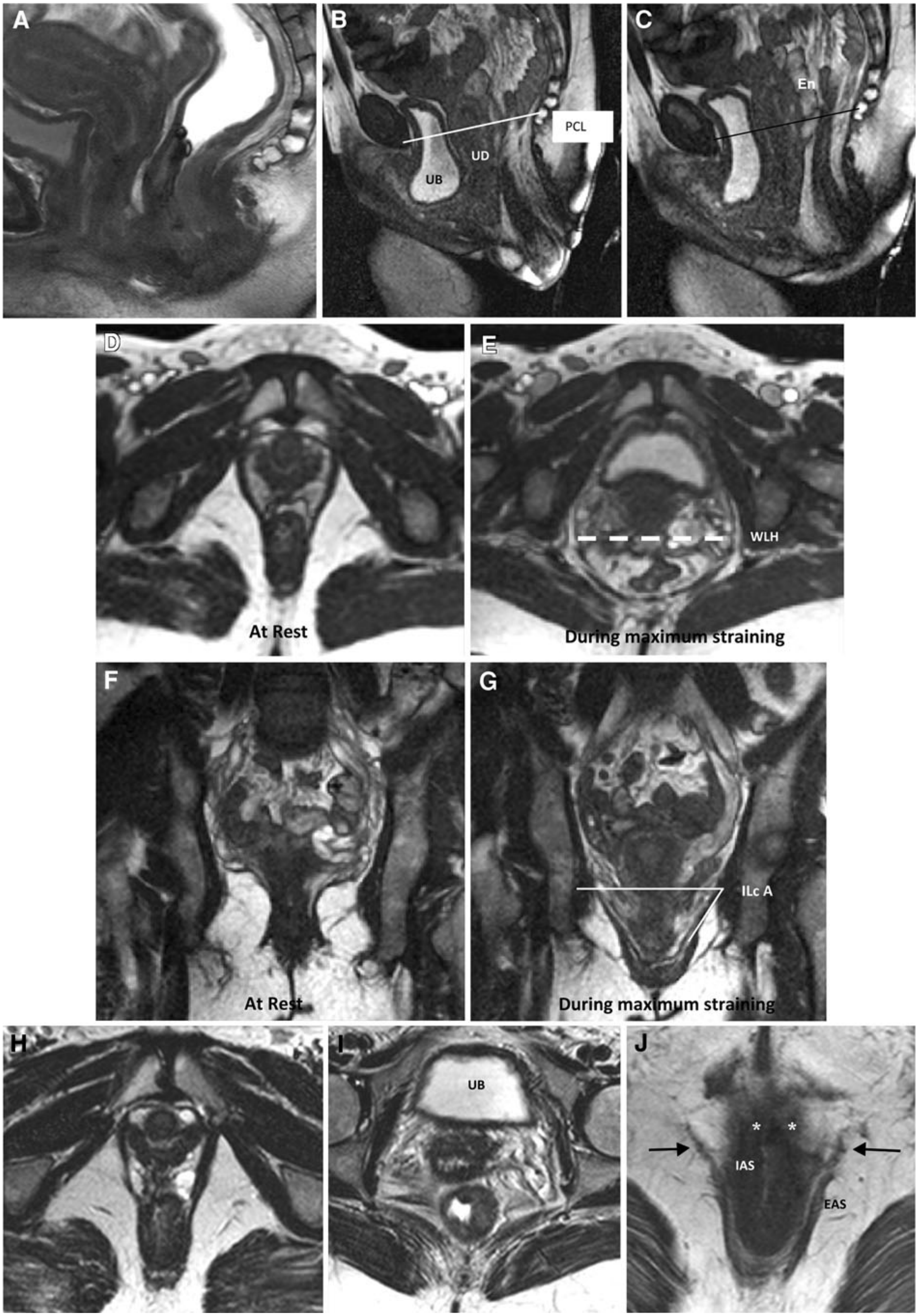
A
B
PCL
UD
UB
C
En
D
At Rest
E
WLH
During maximum straining
F
At Rest
G
ILc A
During maximum straining
H
I
UB
J
IAS
EAS

◀ **Fig. 10.** How to report MRI findings in complex cases of PFD as in this patient presenting with POP and anal incontinence. In sagittal BFFE (TR/T 9/4) images (at rest in **A** and during maximum straining in **B** and **C**), the location, type, and grade of prolapse are assessed; from anterior to posterior there are grade II cystocele, uterine descent (UD), grade I enterocele (EN), advanced anorectal junction descent and rectal prolapse. Dynamic **D**, **E** axial and **F**, **G** coronal BFFE images. From these images, the radiologist can measure the width of the levator hiatus (WLH, *dashed line*) and the iliococcygeus angle (Ilc A, *solid line*). **H–J** The corresponding axial T_2-weighted TSE images (5000/132); **H** is at the level of the urethral supporting elements, revealing an intact system, and **I** is at level II endopelvic fascial support showing also a straight posterior urinary bladder wall and hence intact fascia. **J** Axial BFFE (9/4) of the anal sphincter; there is an anterior external anal sphincter (EAS) defect from 10 to 2 o'clock (*arrows*), as well as fraying and fibrosis (**) of the internal anal sphincter (IAS). Through correlation between the static images (**H**, **I**, **J**) and the dynamic images (**A–G**), the predominant underlying structural defect for each of the patient's complaint can be pinpointed. In this case, POP was not due to fascial defect which is intact as shown in **I**, and it is attributed to the predominating pelvic floor muscle weakness as assessed in **B**, **C**, **E**, **G** (and not to tear or defect, because the muscle attachments were intact). Anal incontinence was due to anal sphincter injury as shown in **J**. The possibility of masked stress urinary incontinence (SUI) due to the marked descent of the bladder base with kinking of the urethra was not a concern, because correlation with static images revealed a normal urethral supporting system that is assessed in **H**. At a follow-up examination 1 year after repair of POP and the anal sphincter, the patient did not report the appearance of masked SUI. *UB* urinary bladder, *UD* uterine descent.

diameter of the muscle reflects the extent of its ballooning during straining. It rarely exceeds 4.5 cm in women with an intact pelvic floor [6, 36].

On the coronal plane, the iliococcygeus angle [54] is measured between the iliococcygeus muscle and the transverse plane of the pelvis in posterior coronal images at the level of the anal canal (Fig. 10F, G). The transverse plane of the pelvis is obtained by joining the corresponding bony landmarks on the pelvic sidewalls at the level of origin of the iliococcygeus muscle from the obturator internus, usually at the level where the complete iliac blades are seen in the coronal plane [6]. This angle reflects the degree of descent and movement of the muscle [54].

Measurements obtained on dynamic images in the three orthogonal planes. In healthy volunteers with no symptoms of lower genitourinary abnormalities, the mean measurements obtained during maximum straining in the three orthogonal planes are as follows: length of the H-line 5.8 ± −0.5 cm, length of the M-line 1.3 ± 0.5 cm, levator plate angle 11.7° ± 4.8°, width of the levator hiatus 4.5 ± 0.7 cm, iliococcygeus angle 33.4° ± 8.2° [6]. These five measurements of supporting structures are all considered to reflect the status and the weakness of the levator ani. They have proven to be of value in identification of pelvic floor laxity and quantification of the degree of weakness. They are also useful for follow-up assessment.

Why correlation between static and dynamic magnetic resonance images could be a good solution

Magnitude of PFD. PFD is a common problem. The most prevalent forms of dysfunction are UI, POP, and anal incontinence, all of which affect women 3–7 times more often than men, at an estimated incidence of 23.7% of women in the United States [55]. Approximately 10%–20% of these patients are symptomatic, and by the age of 70 years, an estimated 1 in 10 undergoes pelvic floor surgical repair. In addition, by 2042, the population of women older than 60 years is expected to increase at a higher rate than the general population, resulting in a projected 45% increase in the demand for all services related to treatment of pelvic floor disorders [56]. With this demographic shift, it is also expected that there will be an increased demand for imaging this population.

Current treatment and reported recurrence rate. Although multiple factors predispose for PFD, the precise pathologic mechanism is poorly understood, and treatment is often started regardless of the specific anatomical lesion involved, possibly because one of the following factors: a lack of understanding of normal anatomy and physiology of the pelvic floor, a lack of solid data on selection criteria for the various surgical techniques, and the sparsity of data on the outcome of different procedures. This situation was reflected in a study by Olsen et al. [4], who reported that 29% of the procedures performed for incontinence and prolapse were reoperations, suggesting the need for advances in both the diagnosis and treatment of these disorders.

The clinician's needs. Several clinicians who specialize in the field of PFD have stated that a "wide variety of surgical procedures have been used, with several based on weak scientific evidence" [27]. In several studies, DeLancey [3, 57] showed, for example, that a common problem such as SUI results from specific damage to muscles, fascial structures, and nerves of the pelvic floor. He suggested that if we begin to define the damage occurring in each element of the continence mechanisms, we should be able to precisely select treatment plans that are based on the abnormality found in individual patients. However, DeLancey cautioned that before these advances can be realized, we must reconsider how we think about this common problem. He noted the value of switching from the current empirical approach to treatment, which is based on a symptom complex that assigns a woman who says she has urine leakage to treatment for

SUI, to a therapeutic model that investigates and is based on the specific neuromuscular and fascial defect that results in the symptom complex. He stated that the optimal approach to treatment must be individualized for each patient on the basis of both the symptom complex and the specific anatomical and structural abnormalities. What had long been missing was a tool for accurately defining the anatomical and structural abnormalities in each patient.

The radiologist's role. All diagnostic modalities, including physical examination and standard MRI assessment, are directed toward two basic goals in the clinical and radiological assessment of POP: first, to determine whether prolapse of specific organ is indeed present and second, to determine the degree of prolapse. However, we believe, as others do [58], that as new modalities of evaluation appear, our concepts of form and function change. Improved imaging of anatomical structures with MRI has allowed superior soft-tissue resolution and consequently provided a more realistic glimpse of the structural relationships in vivo. With changing concepts, it is necessary to reexamine and redefine the underlying anatomy, which requires a functional classification system that is based on scientific evidence. On the basis of the new three-part pelvic supporting system classification developed in my institution, we were able to create a correlative analytical approach that can provide better data for treatment planning.

The basis of this approach is simultaneous analysis of findings obtained from static and dynamic magnetic resonance images of the same patient with correlation with the data obtained to determine whether a particular anatomical defect in the pelvic supporting system detected on static images is associated with a specific dysfunction on dynamic images. The most marked type of defect was reported as the predominant defect (Figs. 7, 9, 10). This correlative analysis between the 2 types of magnetic resonance images made it possible to link PFD to specific structural defects because certain anatomical derangement and abnormalities on static images were found to be associated with specific kinematic dysfunctions. In this context, SUI was found to be associated with structural defects in the urethral supporting elements and not with bladder neck descent [6]. In regard to POP, the usual practice is to lump different types of bladder-based descent under the single term *cystocele*. Cystocele can be documented on sagittal dynamic magnetic resonance images obtained at maximum straining, but it is not possible from these midline images to identify the specific differentiating structural defects [3]. However, the integrated MRI analytical approach makes it possible to differentiate whether POP is caused by defects in the endopelvic fascia, or levator muscle weakness, or instead on abnormalities in both the endopelvic fascia and the levator muscles [6]. Therefore, instead of the clinician focusing on a "dropped bladder," the radiologist can use combined analysis of both kinds of images to provide the clinician with complete mapping of the site and types of defects. Such information may help the clinician decide on physiotherapy for a patient with global muscle weakness and normal fascia, or on surgical repair for a patient with a focal break in the fascia and/or a muscle tear. The main aims of this approach are to increase the success rates for current treatments and to devise new treatments.

Conclusion

The success of advanced pelvic floor imaging for treatment planning will be determined not only by whether treatment is affected by the new information that the imaging modality provides but also by whether this information ultimately reduces complication rates and substantially improves clinical outcomes. Our recently described correlative analytical approach converts static and dynamic MRI from two separate types of images into an integrated system that can more precisely identify the underlying anatomical defect responsible for symptoms in individual patients with PFD, even allowing differentiation of the underlying anatomical defect when any two patients have the same symptoms. This type of information, when reported by the radiologist to the clinician, gives insight into the diagnosis of these complex disorders and makes possible individualized, defect-specific approaches to treatment that may minimize the risk of surgical failure, dysfunction recurrence, and reoperation. Hence, we believe that this approach enhances collaboration and interaction between radiologist and clinician, to the benefit of the patient, as it provides a common language through which the radiologist can effectively communicate imaging findings.

Acknowledgments. Medical editor Katharine O'Moore-Klopf, ELS (East Setauket, NY, USA) provided professional English-language editing of this article.

References

1. Maglinte DDT, Kelvin PM, Fitzgerald K, et al. (1999) Association of compartments defects in pelvic floor dysfunction. AJR Am J Roentgenol 172:439–444
2. Bump RC, Norton PA (1998) Epidemiology and natural history of pelvic floor dysfunction. Obstet Gynecol Clin North Am 25: 723–746
3. DeLancey JO (2005) The hidden epidemic of pelvic floor dysfunction: achievable goals for improved prevention and treatment. Am J Obestet Gynecol 192:1488–1495
4. Olsen AL, Smith VJ, Bergstrom JO, et al. (1997) Epidemiology of surgically managed pelvic organ prolapse and urinary incontinence. Obstet Gynecol 89:501–506
5. Black N, Downs S (1996) The effectiveness of surgery for stress incontinence in women: a systematic review. Br J Urol 78:497–510
6. El Sayed RF, Mashed SE, Farag A, et al. (2008) Pelvic floor dysfunction: assessment with combined analysis of static and dynamic MR imaging findings. Radiology 248:518–530
7. El Sayed RF, Fielding JR, El Mashed S, et al. (2005) Preoperative and postoperative magnetic resonance imaging of female pelvic

floor dysfunction: correlation with clinical findings. J Women's Imaging 7:163–180
8. Kaufman HS, Buller JL, Thompson JR, et al. (2001) Dynamic pelvic magnetic resonance imaging and cystocolpoproctography alter surgical management of pelvic floor disorders. Dis Colon Rectum 44:1575–1584
9. Altringer WE, Saclarides TJ, Dominguez JM, et al. (1995) Four-contrast defecography: pelvic "floor-oscopy". Dis Colon Rectum 38:695–699
10. Strohbehn K (1998) Normal pelvic floor anatomy. Obstet Gynecol Clin North Am 25:683–705
11. DeLancey JO (1994) The anatomy of pelvic floor. Curr Opin Obstet Gynecol 6:313–316
12. Abrams P, Cardozo L, Fall M, et al. (2002) The standardisation of terminology of lower urinary tract function: report from the standardisation sub-committee of the international continence society. Neurourol Urodyn 21:167–178
13. Fultz NH, Burgio K, Diokno AC, et al. (2003) Burden of stress urinary incontinence for community-dwelling women. Am J Obstet Gynecol 189:1275–1282
14. Minassian VA, Drutz HP, Al-Badr A (2003) Urinary incontinence as a worldwide problem. Int J Gynaecol Obstet 82:327–338
15. Hunskaar S, Burgio K, Diokno AC, et al. (2000) Epidemiology and natural history of urinary incontinence. Int Urogynecol J Pelvic Floor Dysfunct 11:301–319
16. Hannestad YS, Rortveit G, Sandvik H, Hunskaar S (2000) A community-based epidemiological survey of female urinary incontinence: the Norwegian EPINCONT study. Epidemiology of Incontinence in the County of Nord-Trøndelag. J Clin Epidemiol 53:1150–1157
17. Jeffcoate TN, Roberts H (1952) Observation on stress incontinence of urine. Am J Obstet Gynecol 64:721–738
18. Enhorning G (1961) Simultaneous recording of intravesical and intra-urethral pressure: a study on urethral closure in normal and stress incontinent women. Acta Chir Scand Suppl 276:1–69
19. Mostwin JL, Yang A, Sanders R, Genadry R (1995) Radiography, sonography, and magnetic resonance imaging for stress urinary incontinence: contributions, uses, and limitations. Urol Clin North Am 22:539–549
20. Kim JK, Kim YJ, Choo MS, Cho KS (2003) The urethra and its supporting structures in women with stress urinary incontinence: MR imaging using an endovaginal coil. AJR Am J Roentgenol 180:1037–1044
21. DeLancey JO (1994) Structural support of the urethra as it relates to stress urinary incontinence: the hammock hypothesis. Am J Obstet Gynecol 170:1713–1720
22. Koelbl H, Mowstin J, Boiteux JP, et al. (2002) Pathophysiology. In: Abrams P, Cardozo L, Koury S, Wein A (eds) *Incontinence*, 2nd edn. Plymouth: Health Publications Ltd, pp 165–201
23. McCarthy TA (1991) Medical history and physical examination. In: Ostergard DR, Bent AE (eds) *Urogynecology and urodynamics: theory and practice*, 3rd edn. Baltimore: Williams & Wilkins, pp 99–101
24. Wall LL, Norton PA, DeLancey JOL (1993) *Practical urogynecology*. Baltimore: Lippincott Williams & Wilkins, pp 83–124
25. Strohbehn K (2003) Urodynamics. In: Bartram CI, DeLancey JO, Halligan S, et al. (eds) *Imaging pelvic floor disorders*. New York: Springer, pp 89–97
26. Coates K (1998) Physiologic evaluation of the pelvic floor. Obstet Gynecol Clin North Am 25:805–824
27. Cardozo L (2004) New developments in the management of stress urinary incontinence. BJU Int 94(suppl 1):1–3
28. Woodfield CA, Krishnamoorthy S, Hampton BS, Brody JM (2010) Imaging pelvic floor disorders: trend toward comprehensive MRI. AJR Am J Roentgenol 194:1640–1649
29. Yang A, Mostwin JL, Rosenshein NB, Zerhouni EA (1991) Pelvic floor descent in women: dynamic evaluation with fast MR imaging and cinematic display. Radiology 179:25–33
30. Mengert WF (1936) Mechanics of uterine support and position. Am J Obstet Gynecol 31:775–782
31. DeLancey JO (1993) Anatomy and biomechanics of genital prolapse. Clin Obstet Gynecol 36:897–909
32. DeLancey JO (2003) Functional anatomy of the pelvic floor. In: Bartram CI, DeLancey JO, Halligan S, et al. (eds) *Imaging pelvic floor disorders*. New York: Springer, pp 27–38
33. Bump RC, Mattiasson A, Bo K, Brubaker LP, et al. (1996) The standardization of terminology female pelvic floor dysfunction. Am J Obstet Gynecol 175:10–17
34. Theofrastous JP, Swift SE (1998) The clinical evaluation of pelvic floor dysfunction. Obstet Gynecol Clin North Am 25:783–804
35. Pannu KH, Kaufman SH, Geoffrey WC, et al. (2000) Dynamic MR imaging of pelvic organ prolapse: spectrum of abnormalities. Radiographics 20:1567–1582
36. Fielding JR (2002) Practical MR imaging of female pelvic floor weakness. Radiographics 22:295–304
37. Kelvin FM, Maglinte DDT, Hale DS, Benson JT (2000) Female pelvic organ prolapse: a comparison of triphasic dynamic MR imaging and triphasic fluoroscopic cystocolpoproctography. AJR Am J Roentgenol 174:81–88
38. Comiter CV, Vasavada SF, Barbaric ZL, et al. (1999) Grading pelvic prolapse and pelvic floor relaxation using dynamic magnetic resonance imaging. Urology 3:454–457
39. Colaiacomo MD, Masselli G, Polettini E, et al. (2009) Dynamic MR imaging of the pelvic floor: a pictorial review. Radiographics 35:1–42
40. Nyagaard IK, Kreder KJ (1994) Complication of incontinence surgery. Int Urogynecol J 5:353–360
41. Singh K, Reid WM, Berger LA (2001) Assessment and grading of pelvic organ prolapse by use of dynamic magnetic resonance imaging. Am J Obstet Gynecol 185:71–77
42. Wall LL (1996) Incontinence, prolapse, and disorders of the pelvic floor. In: Berek JF, Adashi EY, Hillard PA (eds) *Novek gynecology*, 12th edn. Baltimore: Williams & Wilkins, pp 619–676
43. Beco J, Mouchel J (2003) Perineology: a new area. Urogynaecol Int J 17:79–86
44. El Sayed RF (2009) Female pelvic floor dysfunction. In: Morcos SK, Thomsen HS (eds) *Imaging in genitourinary medicine: a problem-oriented approach*. Chichester: Wiley-Blackwell, pp 399–413
45. El Sayed RF, Morsy MM, El Mashed SM, Abdul-Azim MS (2007) Anatomy of the urethral supporting ligaments defined by dissection, histology, and MRI of female cadavers and MRI of healthy nulliparous women. AJR Am J Roentgenol 189:1145–1157
46. Stoker J, Rociu E, Bosch JL, et al. (2003) High-resolution endovaginal MR imaging in stress urinary incontinence. Eur Radiol 13:2031–2037
47. Huddleston HT, Dunnihoo DR, Huddleston PM, Meyers PC (1995) Magnetic resonance imaging of defects in DeLancey's vaginal support levels I, II, and III. Am J Obstet Gynecol 172: 1778–1784
48. DeLancey JO (2002) Fascial and muscular abnormalities in women with urethral hypermobility and anterior vaginal wall prolapse. Am J Obstet Gynecol 187:93–98
49. Lienemann A, Anthuber C, Baron A, et al. (1997) Dynamic MR colpocystorectography assessing pelvic floor descent. Eur Radiol 7:1309–1317
50. Etlik Ö, Arslan H, Odabaşi H, et al. (2005) The role of the MR-fluoroscopy in the diagnosis and staging of the pelvic organ prolapse. Eur J Radiol 53:136–141
51. Cortes E, Reid WMN, Singh K, Berger L (2004) Clinical examination and dynamic magnetic resonance imaging in vaginal vault prolapse. Obstet Gynecol 103:41–46
52. Kelvin FM, Pannu HK (2003) Dynamic cystoproctography: fluoroscopic and MR techniques for evaluating pelvic organ prolapse. In: Bartram CI, DeLancey JO, Halligan S, et al. (eds) *Imaging pelvic floor disorders*. New York: Springer, pp 51–68
53. Goh V, Halligan S, Kaplan G, et al. (2000) Dynamic MRI of the pelvic floor in asymptomatic subjects. AJR Am J Roentgenol 174:661–666
54. Singh K, Reid WM, Berger LA (2002) Magnetic resonance imaging of normal levator ani anatomy and function. Obstet Gynecol 99:433–438
55. Nygaard I, Bradely C, Brandt D (2004) Pelvic organ prolapsed in older women: prevalence and risk factors. Obstet Gynecol 104: 489–497

56. Luber KM, Boero S, Choe JY (2001) The demographics of pelvic floor disorders: current observations and future projections. Am J Obstet Gynecol 184:1496–1501
57. DeLancey JO (1996) Stress urinary incontinence: where are we now, where should we go? Am J Obestet Gynecol 175:311–319
58. Klutke CG, Siegel CL (1995) Functional female pelvic anatomy. Urol Clin N Am 22:487–498
59. Petros PEP (2007) Overview. In: Petros PEP (ed) *The female pelvic floor. Function, dysfunction and management according to the integral theory*, 2nd edn. Berlin: Springer, pp 3–4
60. Hale DS, Kelvin FM, Strohbehn K (2003) Urogenital dysfunction. In: Bartram CI, DeLancey JO, Halligan S, et al. (eds) *Imaging pelvic floor dysfunction*. New York: Springer, p 109
61. Petros PEP (2007) Reconstructive pelvic floor surgery according to the integral theory. In: Petros PEP (ed) *The female pelvic floor: function, dysfunction and management according to the integral theory*, 2nd edn. Berlin: Springer, pp 122–123